Wind Field Deterministic Forecasting

Javier Calvo Sánchez and Gema Morales Martín

Abstract Regional Numerical Weather Prediction (NWP) models are nowadays integrated at resolutions between 1 and 3 km. They are non-hydrostatic models, generally run with explicit deep convection. These models have achieved a significant improvement on high-impact weather simulation comparing with synoptic scale models. Modeling at these scales needs big computer resources. Wind simulations are very sensitive to different features of the model: space resolution, orography representation, surface physiography, and flux exchanges between the surface and the atmosphere. Different formulations and parameterizations are followed to take into account all these topics depending on the stability and the surface properties. This chapter offers a snapshot of how HARMONIE-AROME model deals with these issues to derive a formulation for the 10 m wind.

1 Introduction

Numerical Weather Prediction (NWP) models have improved significantly over the last decades (see Sect. 3). For wind prediction, model resolution is a key aspect. Currently, Limited Area Models (LAM) are run operationally at horizontal resolutions around 1–3 km, but these resolutions may not be enough to represent local wind with complex terrain. There are several methods to further enhance the NWP output but they rely on the quality of the mesoscale model: evolution of the pressure systems, stability of the atmosphere, representation of regional winds and local circulations, etc. When convection takes place, the uncertainty of the model predictions increases and it is recommended to use ensemble methods to estimate the predictability of the forecasts.

J. Calvo Sánchez (✉) · G. Morales Martín
NWP Group of the State Meteorological Agency (AEMET), c/ Leonardo Prieto Castro,
28040 Madrid, Spain
e-mail: fcalvos@aemet.es

G. Morales Martín
e-mail: gmoralesm@aemet.es

R. Perez (ed.), *Wind Field and Solar Radiation Characterization and Forecasting*,
Green Energy and Technology, https://doi.org/10.1007/978-3-319-76876-2_5

2 HARMONIE-AROME Model

The HARMONIE-AROME non-hydrostatic convection-permitting model is a particular configuration of the ALADIN-HIRLAM shared system resulting from the collaboration between ALADIN and HIRLAM Consortia. This configuration described in [4] is based on the AROME-France model [34].

The model performance is very sensitive to the initial state that is estimated by its assimilation system, based on the 3D-Var scheme developed in ALADIN [8], which shares most of the code with the ECMWF and ARPEGE models. A summary of its main features can be found in [17]. A 4DVar system, under construction, will allow to account for flow-dependent forecast errors, improving the use of observations and diminishing model spin up. Moreover, ensemble assimilation techniques are under development. Currently, the analysis of screen level variables is done using a statistical interpolation algorithm [36]. In the near future, assimilation of other soil parameters as soil moisture and leaf area index will be included using an extended Kalman filter approach.

The spectral dynamical core uses a two-time level semi-implicit semi-Lagrangian discretization based on SETTLS approach [19] which allows long time steps (75 s for a 2.5 km resolution). In order to enhance stability, an upper level nesting is applied using Davies relaxation. The non-hydrostatic component is based on ALADIN dynamics [3, 10].

The physics is adapted from Meso-NH research model [7] as it is described in [34]. Surface processes are treated within an externalized surface model called SURFEX [23] (Surface Externalisée, in French), developed by Météo-France in cooperation with the scientific community. Turbulence scheme follows a turbulent kinetic energy approach [13] and convection in the boundary layer uses the EDMF-M scheme which combines eddy diffusivity and mass flux scheme for shallow convection [24, 33]. Deep convection processes are treated explicitly so the microphysics package plays a very important role in the model performance. The package known as ICE3 is a one-moment bulk scheme which uses a three-class ice parametrization [22, 32].

3 Parameterization of Surface Processes. Wind Representation

The surface fluxes which are input to the atmospheric turbulence and radiation schemes are computed within SURFEX [23, 29], which represents surface heterogeneity dividing each grid box in four surfaces (tiles): nature, water (lake), urban areas, and sea. The fraction of each surface is extracted from a global data base named ECOCLIMAP [28]. The fluxes passed to the atmosphere are the averaged fluxes for each subtype weighted by their relative fraction in the grid cell. All the tiles experiment the same forcing by the mean atmospheric variables and radiative fluxes (Fig. 1).

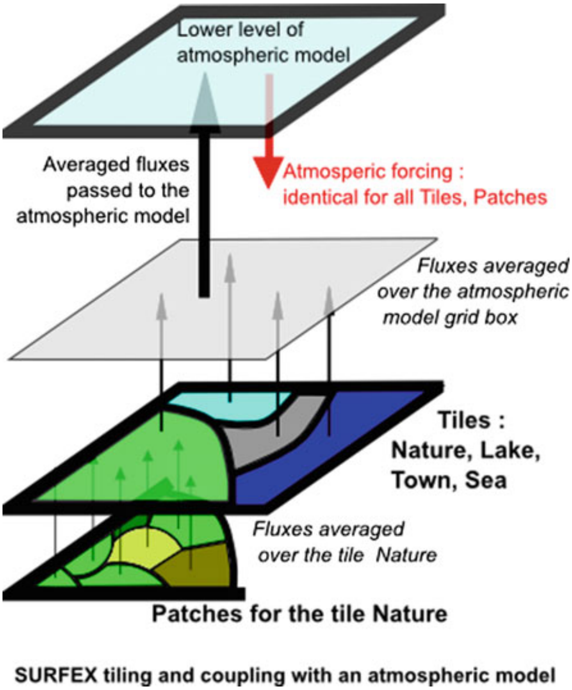

Fig. 1 Tiling approach used in the parameterization of surface processes where fluxes are computed independently in each tile. The grid is divided into 4 tiles and the nature tile is subdivided into 12 patches. The atmosphere feels the averaged fluxes in the grid cell. On the other hand, atmospheric variables and radiative fluxes are sent to the surface where all the tiles receive the same forcing. *Source* CNRM: http://www.umr-cnrm.fr/surfex, [29]

3.1 Soil and Vegetation (ISBA Scheme)

The prognostic equations for surface and soil temperatures and humidities are based on the force-restore method. The soil is divided into several layers including a root zone from which vegetation can extract humidity. Soil freezing effects may play an important role in the energy and humidity fluxes. Vegetation leaves may retain water from precipitation or dew deposition that could be evaporated later. Generally, a one layer snow scheme is used [14].

Following [23], the surface momentum fluxes can be expressed using drag coefficients:

$$\left(\overline{u'w'}\right)_s = -C_D\overline{u}\,|\mathbf{V}| \quad (1)$$

$$\left(\overline{v'w'}\right)_s = -C_D\overline{v}\,|\mathbf{V}| \quad (2)$$

where u, v, w are the wind components, $|\mathbf{V}| = \sqrt{\overline{u}^2 + \overline{v}^2}$ the horizontal wind speed evaluated at first model level, subindex s means evaluated at the surface and C_D a drag coefficient based on Louis formulation [25], modified to consider different roughness lengths for heat z_{0h} and momentum z_0 [26]

$$C_D = C_{DN} F_m \tag{3}$$

where the neutral drag coefficient is

$$C_{DN} = \frac{k^2}{[\ln (z/z_0)]^2} \tag{4}$$

being k the *Von Karmann* constant and the stability function F_m is computed as

$$F_m = 1 - \frac{10 R_i}{1 + C_m \sqrt{|R_i|}} \qquad if \;\; R_i \leq 0 \tag{5}$$

$$F_m = \frac{1}{1 + \frac{10 R_i}{\sqrt{1 + 5 R_i}}} \qquad if \;\; R_i > 0 \tag{6}$$

which are the function of the gradient Richardson number R_i. The coefficient C_m of the unstable case is computed using

$$C_m = 10\, C_m^* C_{DN}\, (z/z_0)^{p_m} \tag{7}$$

$$C_m^* = 6.8741 + 2.6933 \times \mu - 0.3601 \times \mu^2 + 0.0154 \times \mu^3 \tag{8}$$

$$p_m = 0.5233 + 0.0815 \times \mu - 0.0135 \times \mu^2 + 0.0010 \times \mu^3 \tag{9}$$

with

$$\mu = \ln (z/z_{0h}) \tag{10}$$

that depends on roughness lengths for momentum and heat.

Vegetation diversity is represented using 12 vegetation types in three categories:

- Bare soil, rocks, permanent snow and ice (bare soil types).
- C3 crops, C4 crops, irrigated crops, natural herbaceous temperate, natural herbaceous tropics, wetland herbaceous, and irrigated grass (herbaceous types).
- needleleaf trees, evergreen broadleaf trees, and deciduous broadleaf trees (woody trees).

Each vegetation type cover has defined parameters obtained from ECOCLIMAP data base [28]. A summary of the different roughness lengths can be found in Table 1.

Table 1 Roughness lengths for different surface and vegetation types [28]. LAI is the *Leaf Area Index* derived from satellite data and having an annual cycle, h is the typical tree height which is 2 m for bushes and ranges from 15–30 m for forests

Surface/Vegetation type	Roughness length (m)
Sea	$0.015(u_*^2/g)$
Ice/snow	0.0013
Bare soil	0.013
Rocks	0.13
C3 crops	$0.13 \min [1, e^{(LAI-3.5)/1.3}]$
C4 crops and irrigated crops	$0.13 \min [2.5, e^{(LAI-3.5)/1.3}]$
Herbaceous veg	$0.13^{LAI/6}$
Forest	$0.13h$

3.2 Water Surfaces

For sea and lakes, all the prognostic variables are kept constant. The roughness length is given by Charnock's formula:

$$z_{0sea} = 0.015\frac{u_*^2}{g} \tag{11}$$

and with ice ($SST < -2\,°\mathrm{C}$) the roughness length is the one used for snow

$$z_{0ice} = 10^{-3} \tag{12}$$

Momentum fluxes follow Louis approach [25] as described for the ISBA scheme.

3.3 Urban Surfaces

The *Town Energy Budget* (TEB) scheme [27] is based on the canyon approach where the energy budgets are computed for three components: roofs, roads, and walls. If snow is present, two additional budgets are considered for snow on roofs and roads. A spatial average of town characteristics is needed so the parameterization performance is quite sensitive to a proper description of the main town features. The parameters of the scheme depend on building shapes and construction materials.

The problem is that the roughness sublayer can be above the first model level (typically around 10 m). Anyway, the momentum fluxes are computed with the roughness length and the stability coefficients using [26]

$$z_{0town} = \frac{h}{10} \tag{13}$$

where h is the typical building height for the entire surface area with a maximum value of 5 m. There are several types of urban surfaces (dense urban, suburban, urban parks, etc.) each one with specific characteristic parameters.

3.4 Coupling Between the Different Surfaces and the Atmosphere. 10 m Wind

Simple interpolation between the lowest level and the surface
The interpolation is done using Monin Obukov diagnostic profile functions including the roughness length and the surface fluxes computed in the surface parameterization. These wind profile functions follow a logarithmic profile corrected for stability effects (Fig. 2, *left*). The lowest model level is supposed to be high enough to be in the inertial sublayer (constant flux layer). This method is appropriate over the ocean and for homogeneous and smooth surfaces.

Surface Boundary Layer scheme (CANOPY scheme)
Another approach for the surface atmosphere coupling consists on dividing the surface-1st model level layer into different sublayers and run a simplified one column model scheme in these layers [30] (Fig. 2, *right*). In this model, the momentum tendencies and the turbulent kinetic energy tendency have additional terms, function of the LAI, and the vegetation height to account for the vegetation drag.

The same method is also used for urban canopies [18]. This method achieves a finer description of the profiles of the mean variables and fluxes in the surface

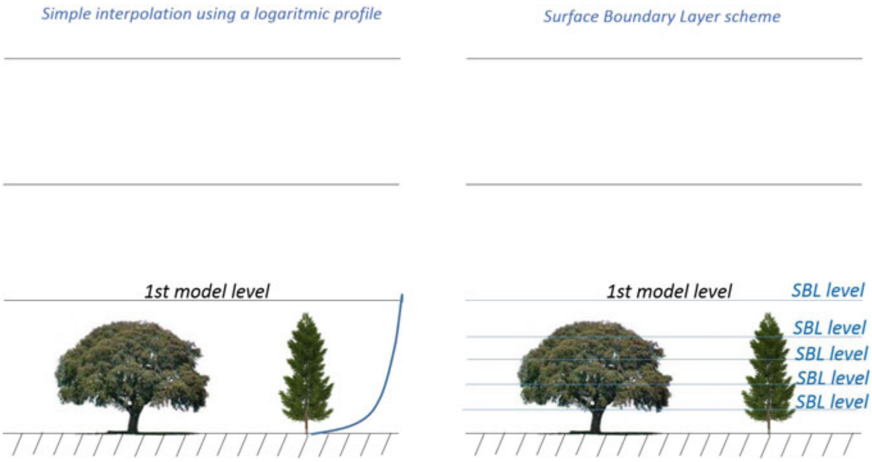

Fig. 2 Coupling between the surface and the first model level using a simple interpolation scheme using a logarithmic profile correcting for stability *(left)* or using the SBL scheme that divides the layer into several sublayers and runs a 1D turbulence scheme accounting for canopy or urban drag *right*

boundary layer that are function of the wind speed and the stability. The method retrieves the logarithmic profile in neutral conditions. In general, it allows a better representation of 2 m variables and 10 m wind. The major improvements are found in stable conditions and for mountainous regions.

3.5 Sub Grid Scale Orography (SSO) Parameterization

There are several options for the orographic drag parameterization in SURFEX. The effects of the small scale orography are parameterized as a momentum sink (drag). The larger scale effects such as mountain blocking and gravity wave breaking are supposed to be resolved at convection-permitting scales (1–3 km resolution).

Z01D
The orographic drag is function of the orographic roughness length z_0 (between 1–60 over orography) that does not depend on wind direction

$$\frac{\partial \left(\overline{u'w'}\right)_{z01D}}{\partial z} = \rho^2 \left[\frac{0.4}{\ln\left(\frac{z}{z_0}\right)}\right]^2 |\mathbf{V}| \tag{14}$$

with z the height of the atmospheric forcing level, $|\mathbf{V}|$ the horizontal wind speed and the roughness length has a maximum value of $z/2$.

Z04D
The same method as *Z01D* but with the roughness length function of the wind direction.

BE04
Following [2], the drag is not function of the roughness but of the sub-grid orography variance σ_{SO}^2

$$\frac{\partial \left(\overline{u'w'}\right)_{BE04}}{\partial z} = C\,\sigma_{SO}^2\, z^{-1.2} e^{-\left[\frac{z}{1500}\right]^{1.5}} |\mathbf{V}| \tag{15}$$

where z is the height, $|\mathbf{V}|$ the horizontal wind speed and the other parameters are constants [2].

Currently, there is no consensus about the benefits of activating the SSO parameterization in HARMONIE-AROME and some operational configurations activate it and others do not.

4 Verification of Operational Wind Forecast

The *State Meteorological Agency of Spain* (AEMET) runs HARMONIE-AROME at 2.5 km horizontal grid spacing over two domains (Iberian Peninsula-Balearic

Islands and the Canary Islands). The vertical discretization includes 65 levels with 15 levels below 1000 m and the model top at 10 hPa. The model analysis updates the atmospheric and surface variables every 3 h using a cutoff time of 1 h and 10 min for the observations, including convectional and aircraft data as well as GNSS zenith total delay and ATOVS satellite data. Other satellite observations and radar data will be included in the near future. The boundary conditions are provided by the ECMWF-IFS integrations corresponding to a cycle 6 h earlier than the Limited Area Model cycle. The HARMONIE-AROME 2.5 km model significantly improves local and extreme forecasts of coarser grid models like HIRLAM or ECMWF [31].

Verification of wind forecast against observations is a key aspect on model validation. In the traditional point verification, model output is interpolated to observation locations and different statistics are computed in order to assess forecast quality [15, 20, 37]. A new model version is only implemented when it is able to improve statistical scores. Comparison of models with different resolutions is a complex issue because double penalty problems take place [15]. A simple way to compare various models or several model versions is comparing the distribution of events in a forecast observation plot as it is done in Fig. 3 for HARMONIE-AROME (HARM) and ECMWF deterministic model. HARM shows a better distribution especially for the strongest winds where ECMWF has a clear tendency to underestimate these events.

Wind velocity shows a clear diurnal cycle as can be seen in Fig. 4 where mean values as function of the hour of the day are plotted for observed values and for several model versions. It should be taken into account that this plot is dominated by low winds that indeed are the ones that occur more frequently.

In order to take into account the uneven distribution of observations, it is very useful to split the verification into different categories corresponding to different intervals of observed wind speed and then compute categorical scores on these intervals. An example of this type of categorical verification is shown in Fig. 5 where Kuiper Skill Score is calculated. HARMONIE-AROME improves ECMWF forecasts for all the forecasting categories.

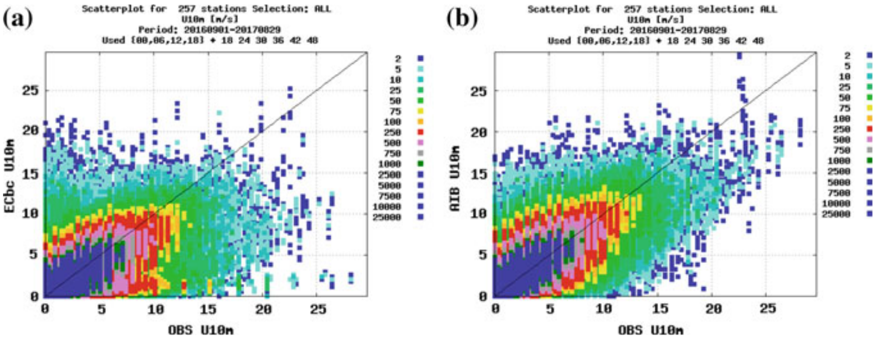

Fig. 3 Comparison of observation forecast events for ECMWF *(upper)* and HARMONIE-AROME *(below)* model for 1 year of forecasts. Narrower distribution and closer to the diagonal implies better forecasts. The biggest differences are found for strong wind cases

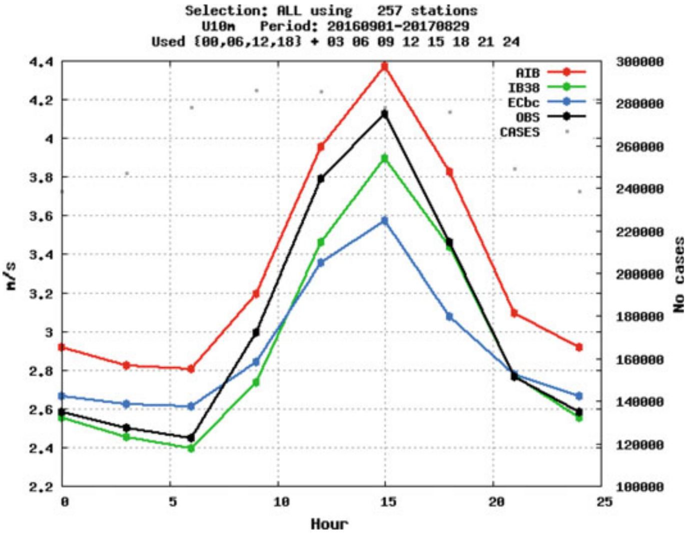

Fig. 4 Comparison of mean values of forecasts and observations plotted as function of the hour of the day showing strongest winds at 15 UTC. Red and green curves correspond to two HARM version whereas green curves correspond to ECMWF forecasts. Basically the models are able to reproduce the diurnal cycle

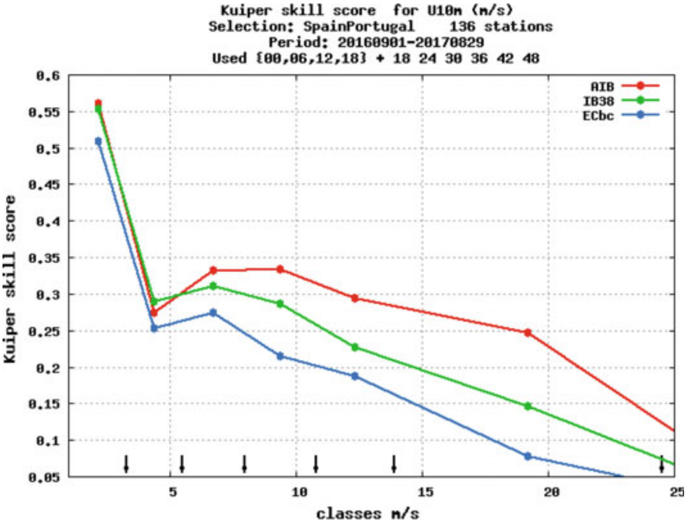

Fig. 5 Kuiper Skil Score comparing ECMWF forecasts *(blue)* with two versions of HARMONIE model (*red* and *green* curves) for 1 year of forecasts. Bigger scores mean better predictions. The differences for wind speeds below 5 m/s are small but the improvement is significant for bigger categories

5 Wind Forecast Case Studies

Mountain ranges exert a significant influence in the atmospheric flow affecting the dynamics of the synoptic systems, producing regional winds and a variety of local effects. Several observation field campaigns have been carried out to improve the understanding of orographic processes [5, 6, 21]. Generally, NWP models use a grid averaged orography what implies a smoothing of the real topographic height and an underestimation of the orographic obstacles. Coarse resolution models, as global models, include a parameterization of orographic processes (blocking effects and breaking of orographic waves) to overcome this limitation. Higher resolution models, as convection-permitting models, resolve better these processes and only include a parameterization for subgrid scale turbulence generated by the topography. Generally, synoptic models (above 10 km resolution) underestimate the orographic drag and the mountain effects [16]. Figure 6 shows a simulation with HIRLAM model at 10 km resolution, using an effective roughness length and no additional parameterization of the orographic processes. The blocking effect of the mountain and regional winds are underestimated in the simulations.

Another example of strong orographic effects took place during the passage of the Tropical Storm Delta over the Canary Islands. In order to simulate this large low pressure system, large modeling domains are necessary and also a good assimilation system, otherwise neither the trajectory nor the intensity can be reproduced. Finally, the major damages in the Islands took place due to downslope windstorms originated

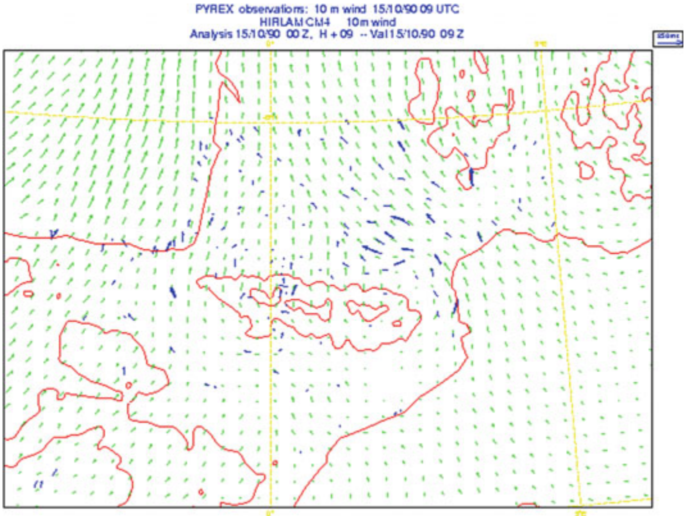

Fig. 6 Comparison of 10 m wind field simulated by HIRLAM model (*green* flags) at 10 km resolution with the observations (*blue*) from the PYREX field campaign [5]. *Red* curves indicate the 1000 and 2000 m topographic height as well as the cost lines. Blocking effects and regional winds are underestimated at this resolution

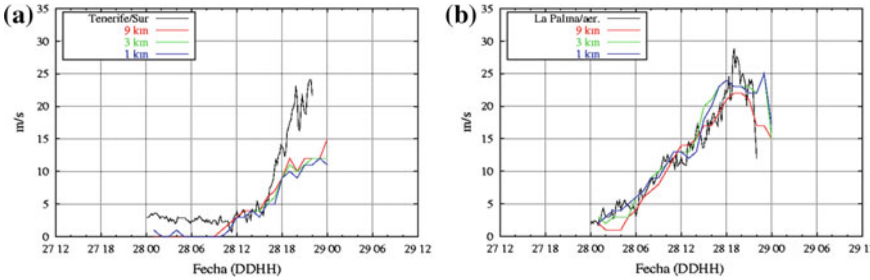

Fig. 7 Comparison of the evolution of the wind speed during 28-11-2005 for two leeward stations (*black*) compared with forecasts at different resolutions. Although the evolution of the wind is generally well represented, the peak in several locations as the Tenerife/Sur station was greatly underestimated even at 1 km resolution

when the flow crossed perpendicularly to the main mountain ranges. Indeed many infrastructures were destroyed and the observations were interrupted due to a generalized power cut. In order to simulate this phenomena, model resolution is a key aspect (Fig. 7):

6 Wind Gust Estimation

Whereas wind field components are forecast variables in the model, wind gust is generally diagnosed using model wind and information from the turbulence scheme [11, 12, 35]. Moreover, the processes leading to gust formation such as deep convection, boundary layer, and orographic processes are generally not well resolved by the models and tend to show a chaotic behavior. Figure 8 shows an example of different methods for estimating gusts associated with the pass of Storm Klaus trough the north of the Iberian Peninsula. The evolution of the gusts is well captured because the evolution of the storm was well reproduced.

However, the errors in the gusts estimation are bigger for purely convective events. Synoptic models use simple parametrization for convective gust but the skill of these estimations is small [1]. On the other hand, convection-permitting models resolve the convective circulations and have more chances of representing better the convective gusts. Nevertheless, at current operational horizontal resolutions, deep convection is not completely resolved what leads to too intense vertical circulations and a general overestimation of the convective gusts.

7 Kilometer and Sub-kilometer Resolutions

Currently, most AROME configurations are run at 2.5 km resolution although Meteo-France is already running the model operationally at 1.3 km including assimilation [9]. Nevertheless, it is important to take into account that the model effective resolution, which is the one of the processes actually resolved, may be six times bigger

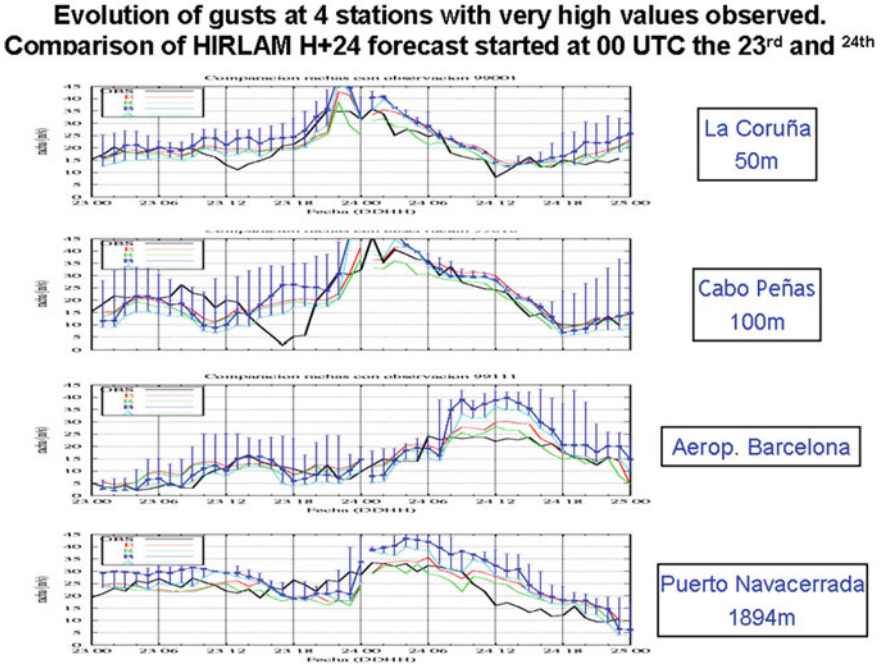

Fig. 8 Extremely intense winds and hurricane force gusts were reported in many places of the Iberian Peninsula when Klaus swept the Peninsula producing several casualties. The model estimate was relatively good because the synoptic evolution of the system was well captured

than the model grid spacing. The AROME system is also run at high resolution in nowcasting mode with very frequent assimilation cycles, going from 10 min to 1 h frequency and performing short forecast lengths (typically up to 6 h). Nowcasting applications normally need ensemble approaches as uncertainty at these scales is big.

Several implementations in the range of 1 km to 500 m are under construction but this is a big challenge because several processes need to be reformulated in the model. At these scales, shallow convection start being resolved by the model (gray scales for shallow convection) so it needs to be redesigned. Besides, to represent turbulence below 500 m, there is need to account for 3D fluxes which implies significant modifications in the current operational codes. Also, the resolution of the physiographic data needs to be enhanced. This includes soil and vegetation characteristics that currently have a resolution around 1 km.

Additionally, high-resolution modeling needs big computer resources, as doubling the model resolution typically implies to increase 8 times the computer cost. Currently, optimization of the models in the context of massive parallel systems is a key aspect and an active field of research (ESCAPE https://www.ecmwf.int/escape and SCALABILITY https://www.ecmwf.int/en/about/what-we-do/scalability programs).

8 Conclusions

Wind simulation has improved significantly using NWP models at convective scales. This is specially the case when orographic processes play an important role. These models generally represent deep convection explicitly having more chances to improve the circulations associated with convection but it should be taken into account that these resolutions are still too broad to resolve completely deep convection. When convection takes place, the predictability decreases and it is advised to follow ensemble approaches to estimate the prediction uncertainty.

The complexity of surface processes is large, in particular in the representation of the wind profile. Different surface covers are taken into account being particularly important the representation of vegetation effects and the presence of water, sea/ice, or urban surfaces. There is no general consensus about the need of an effective roughness length or a subgrid scale orographic parameterization to enhance the orographic effects at convective scale NWP modeling.

References

1. Bechtold P, Bidlot J (2009) Convective gusts. ECMWF, Newsletter No. 119, pp 15–18
2. Beljaars A, Brown R, Wood N (2004) A new parametrization of turbulent orographic form drag. Q J Roy Meteorol Soc 130:1327–1347
3. Bénard P, Vivoda J, Maek J, Smolíková P, Yessad K, Smith C, Broková R, Geleyn J (2010) Dynamical kernel of the Aladin-NH spectral limited-area model: revised formulation and sensitivity experiments. Q J Roy Meteorol Soc 136(646):155–169
4. Bengtsson L, Andrae U, Aspelien T, Batrak Y, Calvo J, de Rooy W, Gleeson E, Hansen-Sass B, Homleid M, Hortal M et al (2017) The HARMONIE-AROME model configuration in the ALADIN-HIRLAM NWP system. Mon Weather Rev 145(5):1919–1935
5. Bougeault P, Benech B, Bessemoulin P, Carissimo B, Jansa A, Pelon J, Petitdidier M, Richard E (1997) PYREX: a summary of findings. Bull Am Meteorol Soc 78(4):637–650
6. Bougeault P, Binder P, Buzzi A, Dirks R, Kuettner J, Houze R, Smith R, Steinacker R, Volkert H (2001) The map special observing period. Bull Am Meteorol Soc 82(3):433–462
7. Bougeault P, Mascart P et al (2009) The Meso-NH atmospheric simulation system: scientific documentation part iii: Physics. Technical Report CNRM. http://mesonh.aero.obs-mip.fr/mesonh/dir_doc/book1_m48_19jan2009/scidoc_p3.pdf
8. Brousseau P, Berre L, Bouttier F, Desroziers G (2011) Background-error covariances for a convective-scale data-assimilation system: AROME-France 3D-Var. Q J Roy Meteorol Soc 137(655):409–422
9. Brousseau P, Seity Y, Ricard D, Lger J (2016) Improvement of the forecast of convective activity from the AROME-France system. Q J Roy Meteorol Soc 142(699):2231–2243
10. Bubnová R, Gwenaëlle H, Bénard P, Geleyn J (1995) Integration of the fully elastic equations cast in the hydrostatic pressure terrain-following coordinate in the framework of the ARPEGE/Aladin NWP system. Mon Weather Rev 123(2):515–535
11. Calvo J, Lopez J, Martín F, Morales G, Pascual R (2009) In: 20th ALADIN workshop and HIRLAM all staff meeting. http://www.umr-cnrm.fr/aladin/IMG/pdf/poster_vientoklaus_final_asm10.pdf
12. Calvo J, Morales G (2009) Verification of wind gust forecasts. In: 19th ALADIN workshop and HIRLAM all staff meeting. http://www.umr-cnrm.fr/aladin/IMG/pdf/ME_JC.pdf

13. Cuxart J, Bougeault P, Redelsperger J (2000) A turbulence scheme allowing for mesoscale and large-eddy simulations. Q J Roy Meteorol Soc 126(562):1–30
14. Douville H, Royer J, Mahfouf J (1995) A new snow parameterization for the Météo-France climate model. Clim Dyn 12(1):21–35
15. Ebert EE (2012) Forecast verification: issues, methods and FAQ. Technical Report WWRP/WGNE Joint Working Group on Forecast Verification Research. http://www.cawcr.gov.au/projects/verification
16. Georgelin M, Bougeault P, Black T, Brzovic N, Buzzi A, Calvo J, Cassé V, Desgagné M, El-Khatib R, Geleyn J, Holt T, Hong SY, Kato T, Katzfey J, Kurihara K, Lacroix B, Lalaurette F, Lemaitre Y, Mailhot J, Majewski D, Malguzzi P, Masson V, McGregor J, Minguzzi E, Paccagnella T, Wilson C (2000) The second compare exercise: a model intercomparison using a case of a typical mesoscale orographic flow, the PYREX iop3. Q J Roy Meteorol Soc 126(564):991–1029
17. Gustafsson N, Janjić T, Schraff C, Leuenberger D, Weissman M, Reich H, Brousseau P, Montmerle T, Wattrelot E, Buánek A, Mile M, Hamdi R, Lindskog M, Barkmeijer J, Dahlbom M, Macpherson B, Ballard S, Inverarity G, Carley J, Alexander C, Dowell D, Liu S, Ikuta Y, Fujita T Survey of data assimilation methods for convective-scale numerical weather prediction at operational centres. Q J Roy Meteorol Soc
18. Hamdi R, Masson V (2008) Inclusion of a drag approach in the Town energy Balance (TEB) Scheme: offline 1D evaluation in a street canyon. J Appl Meteorol Climatol 47(10):2627–2644
19. Hortal M (2002) The development and testing of a new two-time-level semi-lagrangian scheme (SETTLS) in the ECMWF forecast model. Q J Roy Meteorol Soc 128(583):1671–1687
20. Jolliffe I, Stephenson D (2003) Forecast verification: a practitioner's guide in atmospheric science. Wiley
21. Kuettner J (1986) The aim and conduct of ALPEX. Scientific results of the Alpine Experiment. Technical Report GARP Publications Series No. 27, WMO/TD 108, 314
22. Lascaux F, Richard E, Pinty J (2006) Numerical simulations of three different MAP IOPs and the associated microphysical processes. Q J Roy Meteorol Soc 132(619):1907–1926
23. Le Moigne P (2012) SURFEX. scientific documentation. Technical Report CNRM. http://www.umr-cnrm.fr/surfex/IMG/pdf/surfex_scidoc_v2-2.pdf
24. Lenderink G, Holtslag AAM (2004) An updated length-scale formulation for turbulent mixing in clear and cloudy boundary layers. Q J Roy Meteorol Soc 130(604):3405–3427
25. Louis J (1979) A parametric model of vertical eddy fluxes in the atmosphere. Bound Layer Meteorol 17(2):187–202
26. Mascart P, Noilhan J, Hervé G (1995) A modified parameterization of flux-profile relationships in the surface layer using different roughness length values for heat and momentum. Bound Layer Meteorol 72(4):331–344
27. Masson V (2000) A physically-based scheme for the urban energy budget in atmospheric models. Bound Layer Meteorol 94(3):357–397
28. Masson V, Champeaux JL, Chauvin F, Meriguet C, Lacaze R (2003) A global database of land surface parameters at 1-km resolution in meteorological and climate models. J Clim 16(9):1261–1282
29. Masson V, Le Moigne P, Martín E, Faroux S, Alias A, Alkama R, Belamari S, Barbu A, Boone A, Bouyssel, F, Brousseau P, Brun E, Calvet JC, Carrer D, Decharme B, Delire C, Donier S, Essaouini K, Gibelin AL, Giordani H, Habets F, Jidane M, Kerdraon G, Kourzeneva E, Lafaysse M, Lafont S, Lebeaupin Brossier C, Lemonsu A, Mahfouf JF, Marguinaud P, Mokhtari M, Morin S, Pigeon G, Salgado R, Seity Y, Taillefer F, Tanguy G, Tulet P, Vincendon B, Vionnet V, Voldoire A (2013) The surfexv7.2 land and ocean surface platform for coupled or offline simulation of earth surface variables and fluxes. Geosci Model Dev 6(4):929–960. https://doi.org/10.5194/gmd-6-929-2013. https://www.geosci-model-dev.net/6/929/2013/
30. Masson V, Seity Y (2009) Including atmospheric layers in vegetation and urban offline surface schemes. J Appl Meteorol Climatol 48(7):1377–1397
31. Navascués B, Calvo J, Morales G et al (2013) Long-term verification of HIRLAM and ECMWF forecasts over Southern Europe: history and perspectives of numerical weather prediction at AEMET. Atmos Res 125–126(Supplement C), 20–33

32. Pinty J, Jabouille P (1998) A mixed–phase cloud parameterization for use in mesoscale non-hydrostatic model: simulations of a squall line and of orographic precipitations. In: Conference on cloud physics, pp 217–220. American Meteorological Society, Everett, WA (1998)
33. de Rooy WC, de Vries H (2017) Technical Report HIRLAM Technical Report
34. Seity Y, Brousseau P, Malardel S, Hello G, Bénard P, Bouttier F, Lac C, Masson V (2011) The AROME-France convective-scale operational model. Mon Weather Rev 139(3):976–991
35. Sheridan P (2011) Review of techniques and research for gust forecasting and parameterisation. Technical Report, Forecasting Research Technical Report 570, Met Office
36. Taillefer (2002) CANARI - Technical Documentation - Based on ARPEGE cycle CY25T1 (AL25T1 for ALADIN). In: CNRM/GMAP. http://www.umr-cnrm.fr/gmapdoc/spip.php?article3
37. Wilks D (2011) Statistical methods in the atmospheric sciences. Academic Press